Supplement of Atmos. Chem. Phys., 16, 9003–9018, 2016
http://www.atmos-chem-phys.net/16/9003/2016/
doi:10.5194/acp-16-9003-2016-supplement

Atmospheric Chemistry and Physics
Open Access

Supplement of

Linking variations in sea spray aerosol particle hygroscopicity to composition during two microcosm experiments

Sara D. Forestieri et al.

Correspondence to: Christopher D. Cappa (cdcappa@ucdavis.edu)

Table S1. Summary of uncertainties for growth factor (GF) retrieval.

Parameter	Default Value	Perturbation	ΔGF	% ΔGF
f(RH)	3.7	0.5 (7%)	0.05	2.6%
Relative Humidity	85%	1.2%/0.03% (see Table 2)	0.05/0.01[$]	2.4%/0.5%
Refractive Index	1.55	0.04	0.05	2.7%
Particle Diameter	Distribution with mode = ~112 nm	+1%	0.01	<1%

[$] ΔGF values were calculated using Kappa-Kohler equation and assuming a κ value of 1.3 [*Petters and Kreidenweis*, 2007].

Table S2. Measured and actual GFs for pure substances and the implied error in the measured RH.

	Observed	Actual	ΔRH
NaCl	2.09	2.1	0.03%
Ammonium Sulfate	1.59	1.55	1.2%

Uncertainties in the measured f(RH), relative humidity, refractive index, and diameter that contribute to the overall uncertainty in GF retrieval are provided in Table S1. The uncertainty in the CRD extinction is ~5% at 532 nm and the fundamental performance of the CRD method for wet particles is not changed. Therefore, the propagated uncertainty of f(RH) (=$bext_{wet}/bext_{dry}$) = $\sqrt{0.05^2 + 0.05^2}$ = 7%. Two estimates for uncertainty in relative humidity were based on the hygroscopic growth factors of pure NaCl and pure ammonium sulfate generated from a TSI atomizer. The measured values were compared to literature values to infer the error in RH (see Table 2). The refractive index used in this study is appropriate for NaCl. However, refractive index of sea salt mixed with marine derived organic matter is not well known, but a value of 1.48 reported by Nessler et al. [2005] for organic matter has been used in many recent studies [*Partanen et al.*, 2014; *Vaishya et al.*, 2013] for marine derived organic matter. The refractive index of the mixture is likely to be somewhere in between. Assuming that organic matter is 50% of the particles by volume (consistent with the ensemble average fraction reported in this manuscript), the volumeweighted refractive index is 1.51. GF values were retrieved with a refractive index of 1.51 and compared to the GF values retrieved using the default value of 1.55 to assess the uncertainty in the refractive index. The uncertainty of 1% for the measured diameter was determined during the experiments in which a 2nd DMA size-selected particles 100-300 nm.

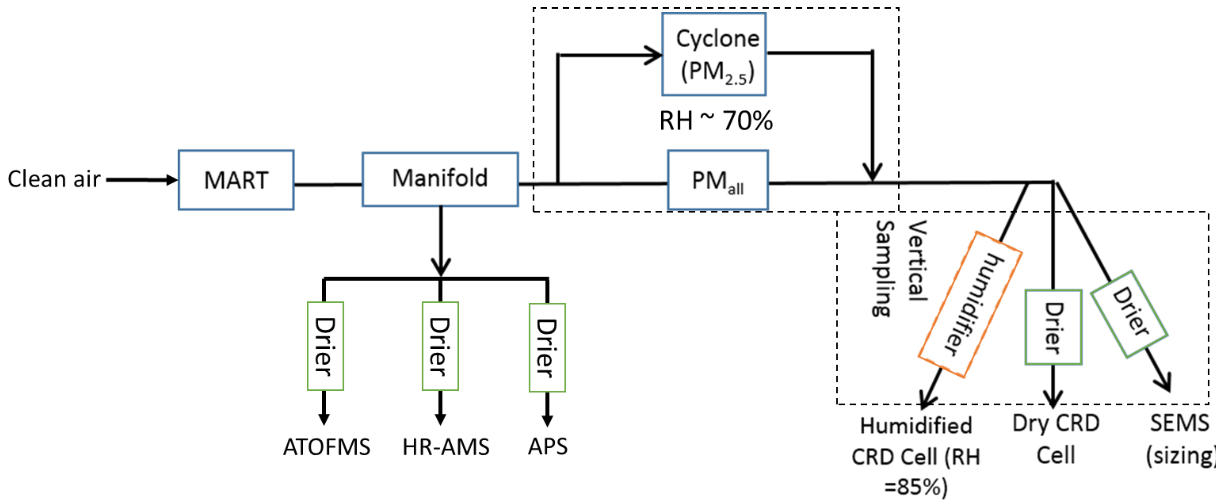

Figure S1. A detailed schematic of the general sampling scheme for the online instruments. Note that not all instruments sampled at the same time (see Table 1). Particles sampled from the MART passed through a manifold from which they were subsampled to the various instrumentation. All instruments included an upstream drier and sampled dried particles. The driers and humidifiers for the CRD and SEMS sampling group (Group 1) were oriented vertically. The particles sampled to the CRD and SEMS alternately passed through a $PM_{2.5}$ cyclone. The RH at this point was ~70%.

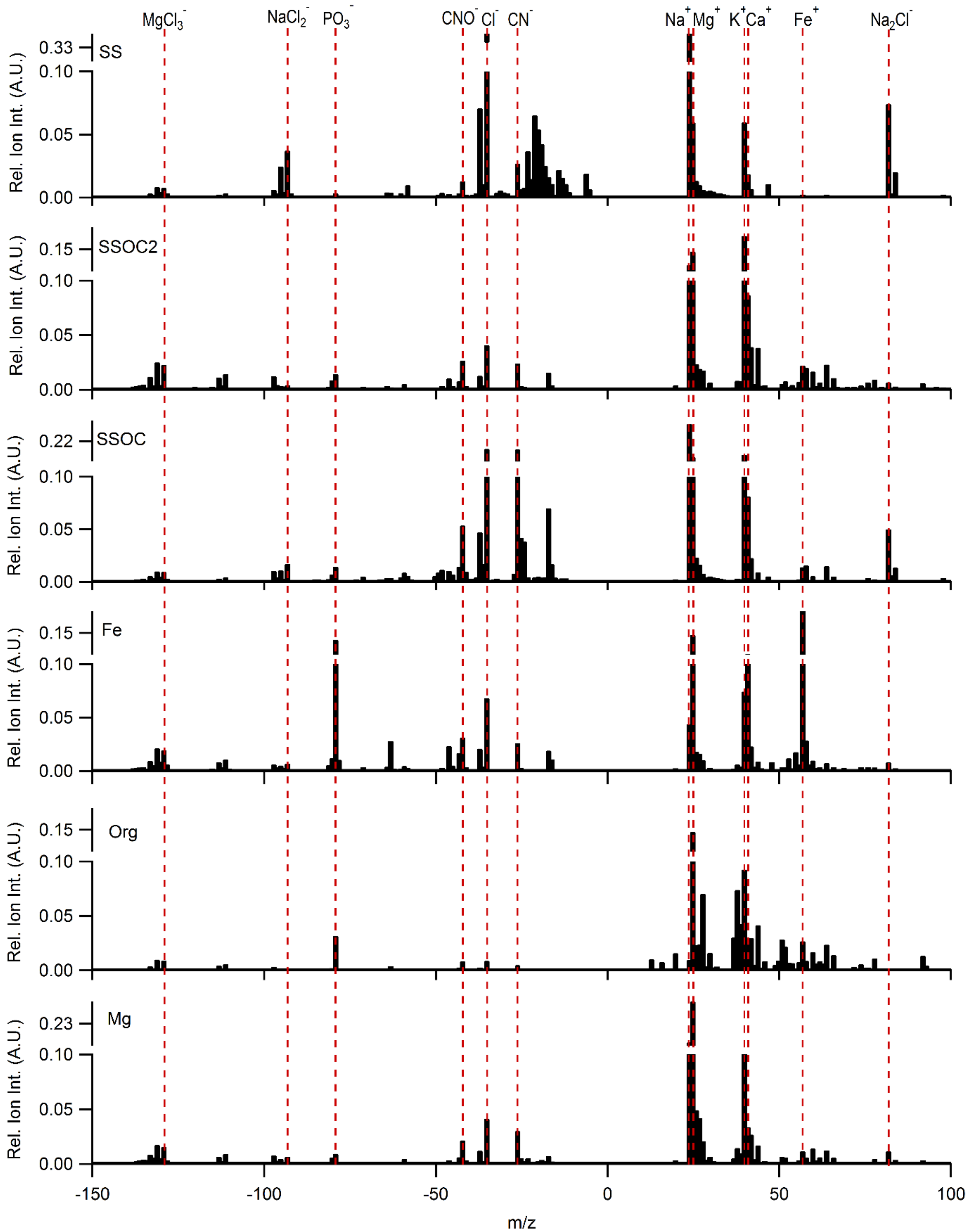

Figure S2. Dual polarity ATOFMS Mass Spectra for the major spectra categories: sea salt (SS), sea salt with organic carbon (SSOC and SSOC2), Iron (Fe), Organic (Org), and Magnesium (Mg) types.

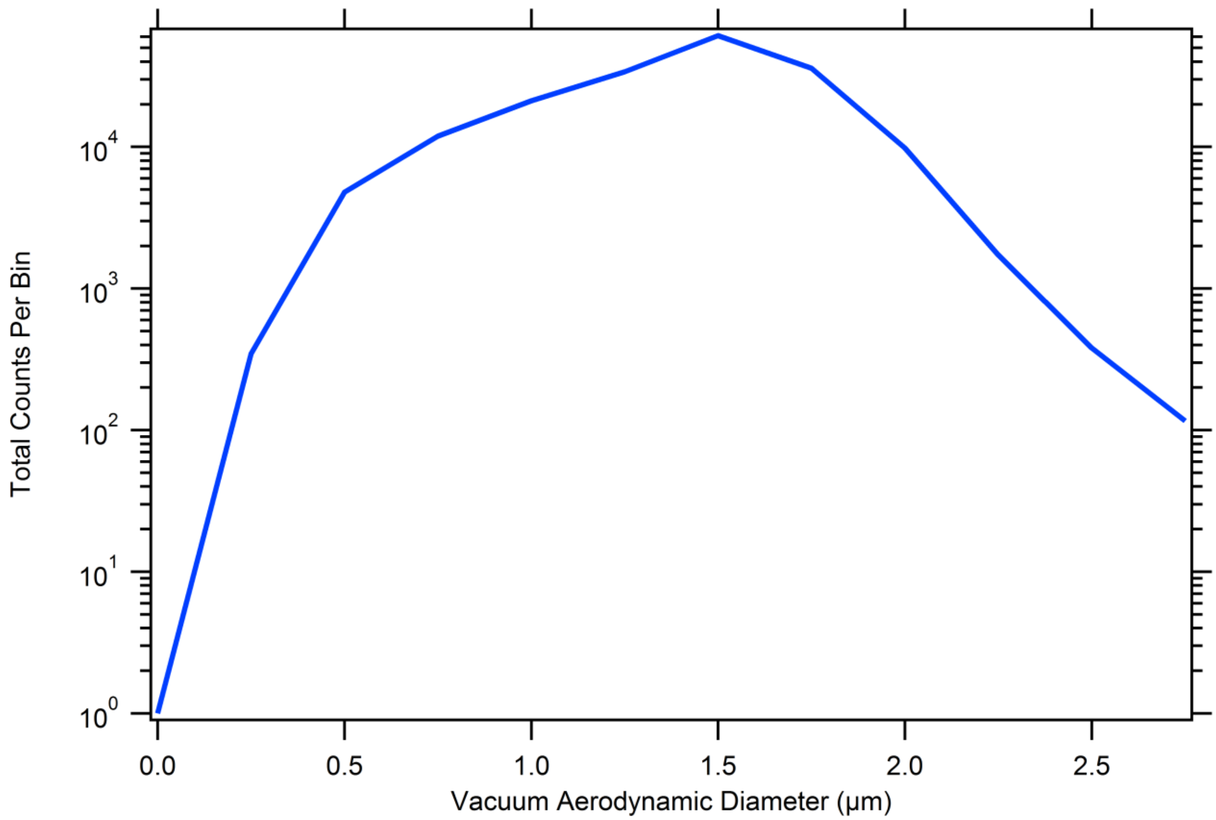

Figure S3. Size-resolved ATOFMS particle counts.

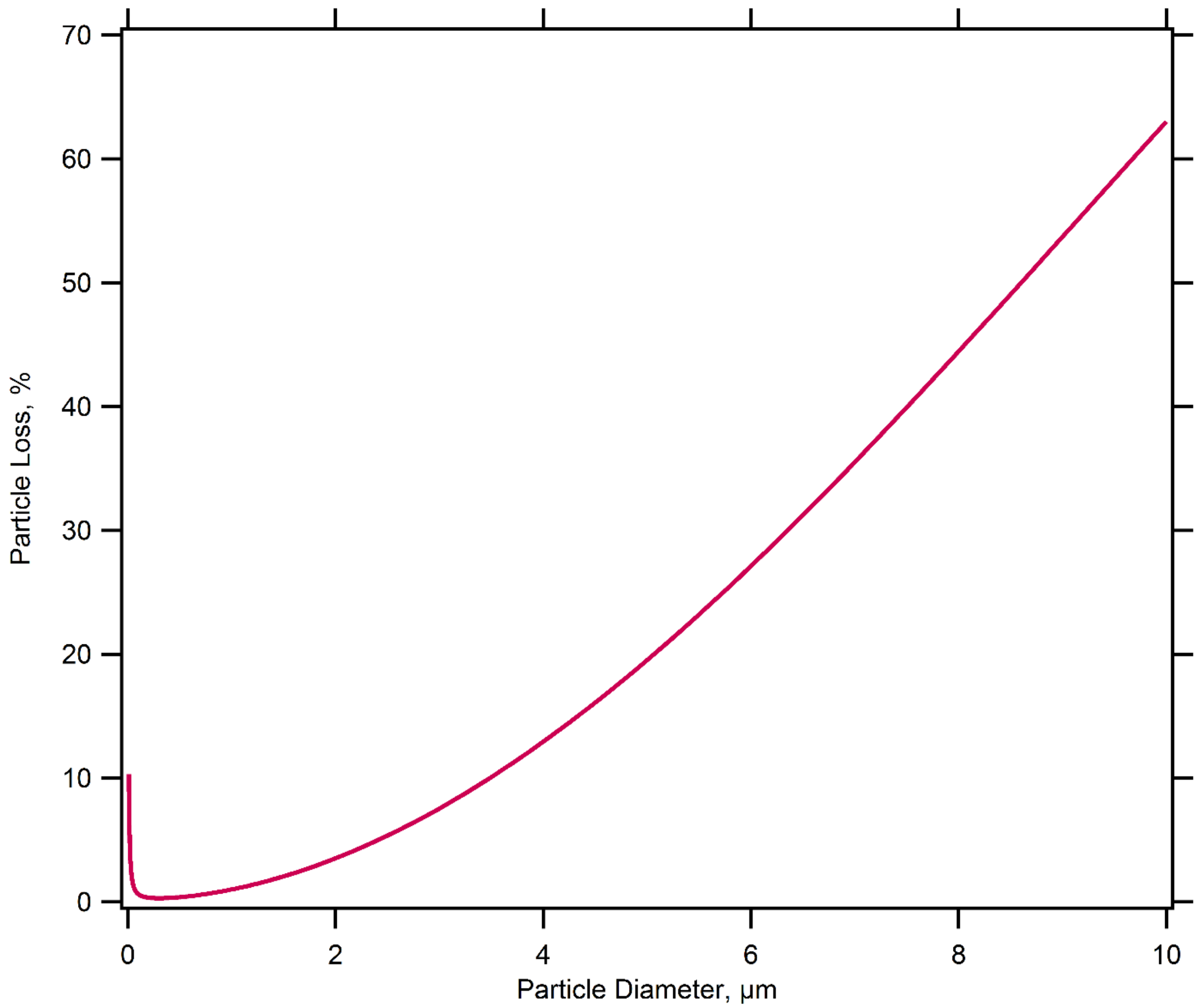

Figure S4. Predicted particle losses for particles travelling from the MART outlet to the MART manifold for a sampling line 10’ in length and 3/8” in diameter. The Particle Loss Calculator of [*Von der Weiden et al.*, 2009] was used.

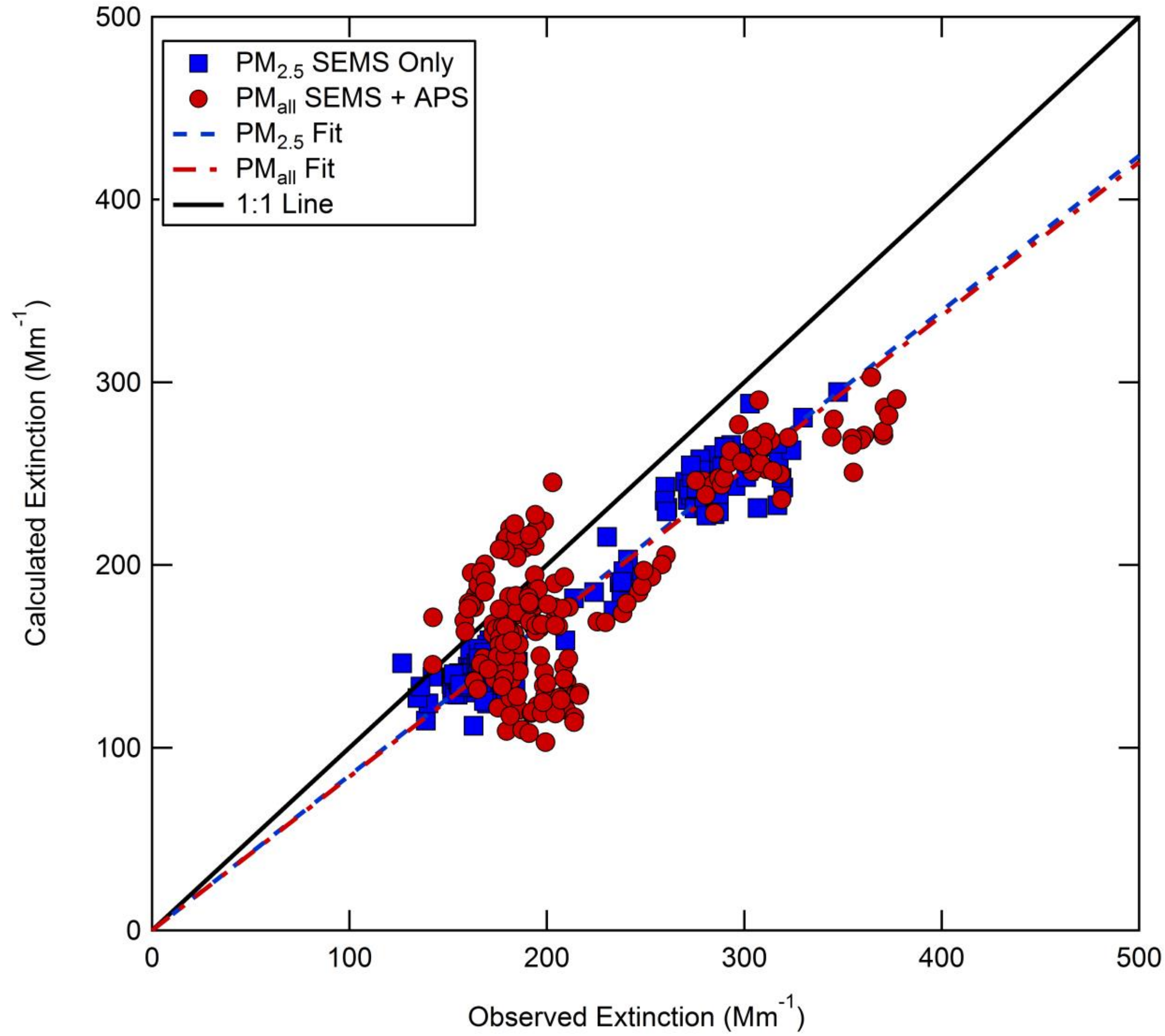

Figure S5. Calculated extinction using SEMS size distributions (real RI = 1.55) for $PM_{2.5}$ and SEMS+APS size distributions as a function of the observed CRD extinction for the 2014 MART experiments. Slopes for linear fits (with the intercept fixed at 0) of calculated extinction as a function of observed extinction were 0.85 and 0.84 for $PM_{2.5}$ and PM_{all}, respectively. A 1:1 line is provided for reference.

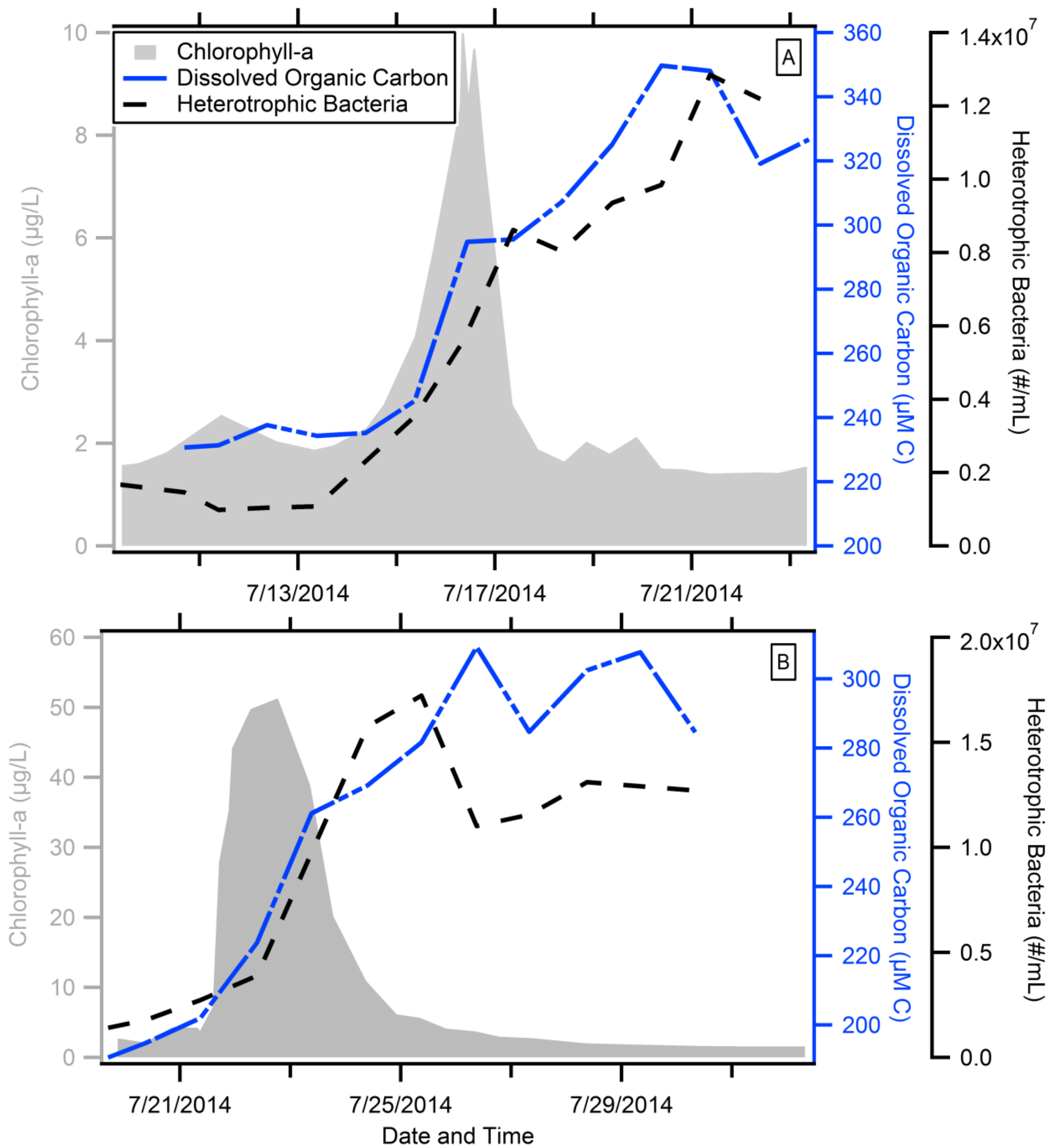

Figure S6. Time series of concentrations of dissolved organic carbon (DOC; µM C), heterotrophic bacteria (#/mL), and chlorophyll-a concentrations (µg/L) in the seawater water for the (A) indoor and (B) outdoor MARTs.

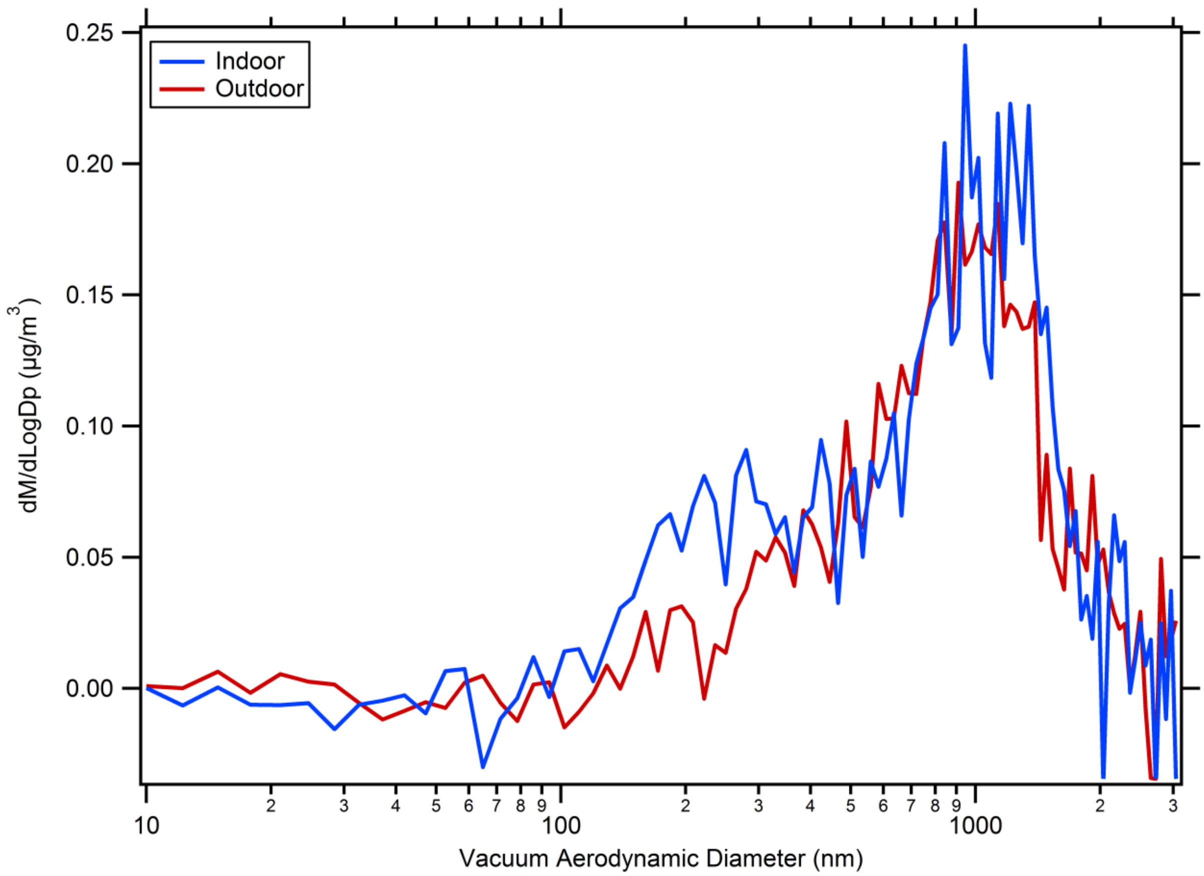

Figure S7. AMS m/z 43 particle time of flight (pTOF) mass distributions for the indoor (blue) and outdoor (red) MARTS.

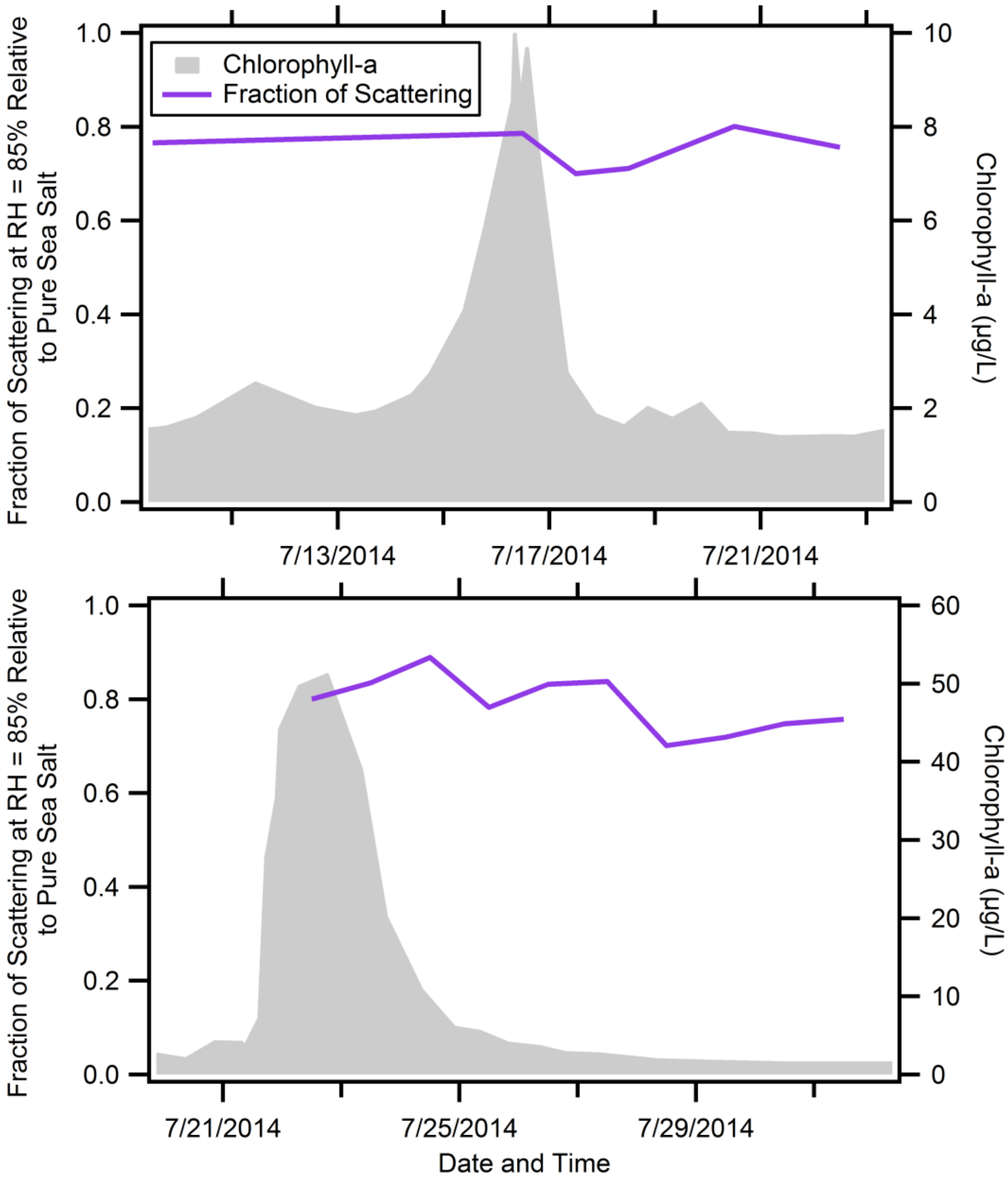

Figure S8. Calculated fraction of scattering relative to pure sea salt particles at 85% RH as a function of time for the two microcosm experiments.

References

DeCarlo, P. F., J. G. Slowik, D. R. Worsnop, P. Davidovits, and J. L. Jimenez (2004), Particle morphology and density characterization by combined mobility and aerodynamic diameter measurements. Part 1: Theory, *Aerosol Science and Technology*, *38*(12), 1185-1205.

Nessler, R., E. Weingartner, and U. Baltensperger (2005), Adaptation of dry nephelometer measurements to ambient conditions at the Jungfraujoch, *Environmental science & technology*, *39*(7), 2219-2228.

Partanen, A. I., et al. (2014), Global modelling of direct and indirect effects of sea spray aerosol using a source function encapsulating wave state, *Atmospheric Chemistry and Physics*, *14*(21), 11731-11752.

Petters, M., and S. Kreidenweis (2007), A single parameter representation of hygroscopic growth and cloud condensation nucleus activity, *Atmospheric Chemistry and Physics*, *7*, 1961-1971.

Vaishya, A., J. Ovadnevaite, J. Bialek, S. G. Jennings, D. Ceburnis, and C. D. O'Dowd (2013), Bistable effect of organic enrichment on sea spray radiative properties, *Geophysical Research Letters*, *40*(24), 6395-6398.

Von der Weiden, S., F. Drewnick, and S. Borrmann (2009), Particle Loss Calculator–a new software tool for the assessment of the performance of aerosol inlet systems, *Atmos. Meas. Tech*, *2*(2), 479-494.